Simulation of atomic ionization following the α decay of the nucleus

2000 J. Phys. A: Math. Gen. 33 5547

(http://iopscience.iop.org/0305-4470/33/31/310)

J. Phys. A: Math. Gen. **33** (2000) 5547–5566. Printed in the UK PII: S0305-4470(00)10681-X

Simulation of atomic ionization following the α decay of the nucleus

F Kataoka†, Y Nogami† and W van Dijk†‡

† Department of Physics and Astronomy, McMaster University, Hamilton, Ontario, Canada L8S 4M1

‡ Redeemer College, Ancaster, Ontario, Canada L9K 1J4

E-mail: vandijk@physics.mcmaster.ca

Received 4 January 2000, in final form 7 June 2000

Abstract. When the nucleus of an atom decays by emitting an α particle, the surrounding electrons are perturbed and the atom may be ionized. We consider two types of schematic one-dimensional models, I and II, that simulate this ionization process. In model I the α particle is treated as a classical point charge that is emitted by the nucleus at a certain time and travels out at constant speed. This model simulates Migdal's method, on which virtually all calculations performed so far for the ionization process are based. Migdal's method yields an ionization probability that is in reasonable agreement with experiment. In model II, the α particle is treated as a quantum mechanical wave that slowly leaks out from the nucleus. The ionization probability that follows from model II, however, is far smaller than that of model I. Implications of this difference are discussed.

1. Introduction

When the nucleus of an atom decays by emitting an α particle, the surrounding electrons are perturbed and the atom may be ionized. This is a very old problem but there remains a curious aspect that is still not well understood.

In 1941 Migdal proposed a method for calculating the ionization probability [1]. Migdal assumed that the α particle emerges from the nuclear surface at a certain time, say $t = 0$, and travels outwards. He treated the α particle as a point charge that obeys a classical equation of motion. The nuclear charge number decreases from Z to $Z - 2$ suddenly at $t = 0$. The surrounding electrons are perturbed by the moving α particle and the sudden change in the nuclear charge. Migdal's pioneering work set a foundation on which virtually all the later calculations for the ionization process are based [2, 3]. Although there have been many improvements, the basic assumption that the α particle can be treated as a classical particle has remained in all of those calculations. Migdal's theory and experiment are in reasonable agreement.

Ideally the α particle should be treated quantum mechanically. According to the model of α decay, proposed by Gamow [4] and by Condon and Gurney [5], the α particle is initially confined within a nucleus and it slowly leaks out, tunnelling through the repulsive Coulomb barrier. The model gives a simple and convincing explanation of the exponential decay law. In this interpretation the rate at which the quantum mechanical wave associated with the α particle leaks out from the nucleus is characterized by the decay half-life, which is usually very long on the atomic time scale. The nuclear charge number changes from Z to $Z - 2$ also

0305-4470/00/315547+20$30.00

at the same slow rate. If we take this picture of the α-decay process, the perturbation on the electrons is almost adiabatic. Consequently the ionization probability that follows from this model will be very small. How can this be consistent with the results of Migdal's method? This is the curious aspect of the process that we mentioned in the first paragraph.

The purpose of this paper is to gain insight into the problem by means of simple schematic models in one dimension that simulate the ionization process. We are interested in the conceptual aspect of the problem rather than the detailed realistic description of the decay process. We consider two models. The first model, which we label model I, simulates Migdal's method. In it we treat the α particle as a classical point particle. In the second model, model II, the α particle is represented by a quantum mechanical wave that slowly leaks out from the nucleus. We find that the two models indeed lead to very different consequences. We discuss implications of this difference.

In section 2 we set up the two models. In section 3 we show the calculations and results of the two models. The models are constructed in such a way that the atom is ionized only through the interaction between the electron and α particle. In section 4 we consider variants of the models which include the effects of the change in the nuclear charge. A summary and a discussion are given in section 5. Some details of the calculations are relegated to appendix A. In appendix B we examine a schematic model for atomic ionization caused by a bombarding α particle. This problem has some, although limited, relevance to the subject of the main text.

2. Models

We consider two one-dimensional models for atomic ionization due to nuclear α decay. Each model consists of an 'atom' and an α-decaying 'nucleus'. For simplicity we assume that the atom has only one 'electron', and that the nucleus is fixed at the origin. In this section we present the models; the details of the calculations will be given in section 3.

Let us begin with model I. We treat the α particle as a classical point particle that is emitted by the nucleus at $t = 0$ and travels at constant speed v_α in the positive x direction. The electron is subject to two interactions, one with the nucleus and the other with the moving α particle. In the actual case these interactions are coulombic but in our model we assume simple artificial interactions. The Hamiltonian for the electron is

$$H_{\mathrm{I}} = H_{\mathrm{e}} + V(x_{\mathrm{e}}, x_\alpha) \tag{2.1}$$

where

$$H_{\mathrm{e}} = \frac{{p_{\mathrm{e}}}^2}{2m_{\mathrm{e}}} + U_{\mathrm{e}}(x_{\mathrm{e}}). \tag{2.2}$$

The subscripts e and α refer to the electron and the α particle, respectively. H_{e} is the Hamiltonian of the model atom with the daughter nucleus. Potential U_{e} is due to the nucleus after the α particle has left, and potential V represents the interaction between the electron and the α particle. We consider only the half-space of $x > 0$ and assume that the electron wavefunction vanishes at $x = 0$.

For U_{e} we assume the following Pöschl–Teller potential [6, 7]:

$$U_{\mathrm{e}}(x_{\mathrm{e}}) = -\frac{(\hbar\lambda)^2}{2m_{\mathrm{e}}} \frac{N(N+1)}{\cosh^2 \lambda x_{\mathrm{e}}} \tag{2.3}$$

where λ are N are constants. The atomic states (in the absence of the α particle) are determined by the Schrödinger equation for stationary states,

$$(H_{\mathrm{e}} - \epsilon_n)\chi_n(x_{\mathrm{e}}) = 0 \qquad \chi_n(0) = 0 \tag{2.4}$$

which can be solved analytically. We assume that N is an integer because then the solutions are particularly simple. The energy eigenvalues are given by

$$\epsilon_n = -\frac{(\hbar\lambda)^2}{2m_e}(N-n)^2 \tag{2.5}$$

where n ($n < N$) is a non-negative integer. The boundary condition $\chi_n(0) = 0$ restricts the values of n to odd integers. For N we take $N = 4$, in which case there are two bound states with $n = 1$ and 3. In addition there are scattering states with continuous energy ϵ, which we denote with $\chi_\epsilon(x_e)$. We give explicit expressions for the wavefunctions for the bound and scattering states in appendix A.

For $V(x_e, x_\alpha)$ we assume an attractive δ-function potential,

$$V(x_e, x_\alpha) = -g\delta(x_e - x_\alpha) \tag{2.6}$$

where $g > 0$ is a constant. It is known that the δ-function potential can be taken as a one-dimensional simulation of the Coulomb potential, see, e.g., [8,9]. We do not use a potential of the form of $1/|x|$ because it exhibits rather strange features, see [10] and references therein. In the numerical illustrations we also examine a smeared-out version of the δ-function potential. (We did not assume a δ-function potential for U_e because we wanted to have more than one bound states.) The α particle is a classical point particle that moves at constant speed v_α,

$$x_\alpha = v_\alpha t \qquad t > 0. \tag{2.7}$$

Then (2.6) becomes $V(x_e, x_\alpha) = -g\delta(x_e - v_\alpha t)$, which is a time-dependent potential experienced by the electron.

The wavefunction of the electron $\psi(x_e, t)$ for $t > 0$ is determined by the time-dependent Schrödinger equation

$$\left(\mathrm{i}\hbar\frac{\partial}{\partial t} - H_I\right)\psi(x_e, t) = 0 \tag{2.8}$$

together with the condition that the electron is in the ground state at $t = 0$,

$$\psi(x_e, 0) = \chi_1(x_e). \tag{2.9}$$

The mass of the α particle does not appear in (2.8).

The electronic transitions are caused by $V(x_e, x_\alpha)$. This model and also model II given below as such do not simulate the effect due to the change in nuclear charge, since we have assumed that the electron wavefunction vanishes at $x = 0$, where the nucleus is located. In section 4 we examine variants of the models, with a different boundary condition such that the effect of the change in the nuclear charge can be simulated.

The atomic transition probability from state 1 to state n is given by

$$p_n(t) = \left|\int_0^\infty \mathrm{d}x_e\, \chi_n^*(x_e)\psi(x_e, t)\right|^2. \tag{2.10}$$

The probability $p_\epsilon(t)\,\mathrm{d}\epsilon$ for transition to the continuum state of energy between ϵ and $\epsilon+\mathrm{d}\epsilon$ can be calculated by replacing $\chi_n(x_e)$ with $\chi_\epsilon(x_e)$ and multiplying the expression corresponding to (2.10) by $\mathrm{d}\epsilon$. For the bound states we actually have only $n = 1$ and 3. Note that, since initially the atom is in the ground state, $p_1(0) = 1$ and $p_3(0) = p_\epsilon(0) = 0$. For $t \gg 1/(\lambda v_\alpha)$ where $1/\lambda$ is of the order of the radius of the model atom, we will find that $p_n(t) \approx p_n(\infty)$. These probabilities all add up to unity,

$$\sum_{n=1,3} p_n(t) + p_{\mathrm{inz}}(t) = 1 \qquad \text{where} \quad p_{\mathrm{inz}}(t) = \int_0^\infty \mathrm{d}\epsilon\; p_\epsilon(t). \tag{2.11}$$

We compare these transition probabilities with their counterparts of model II. In doing so we recall that, although we assumed above that the α particle is emitted at $t = 0$, actually the α particle may be emitted any time. It is understood, however, that the probability for the emission to occur in the time interval from t' to $t' + \Delta t'$ is $(\Gamma/\hbar)\mathrm{e}^{-\Gamma t'/\hbar}\Delta t'$. Therefore it makes more sense to consider the probability that the electron is in state n at time t to be

$$P_n^{\mathrm{I}}(t) = \mathrm{e}^{-\Gamma t/\hbar} p_n(0) + \frac{\Gamma}{\hbar}\int_0^t \mathrm{d}t' \mathrm{e}^{-\Gamma t'/\hbar} p_n(t - t') \tag{2.12}$$

which is a combination of probabilities of two sequential events. The first term on the right-hand side corresponds to the situation where the nucleus has not decayed yet, and the atom remains in the given initial state. The second term consists of a product of two probabilities, one for the emission occurring in the time interval of $\Delta t'$ and the other for the atom being ionized at time t. For the sum of the probabilities defined by equation (2.12) we obtain

$$\sum_{n=1,3} P_n^{\mathrm{I}}(t) + P_{\mathrm{inz}}^{\mathrm{I}}(t) = 1 \qquad \text{where} \quad P_{\mathrm{inz}}^{\mathrm{I}}(t) = \int_0^\infty \mathrm{d}\epsilon\, P_\epsilon^{\mathrm{I}}(t). \tag{2.13}$$

Note that $P_n^{\mathrm{I}}(t) \approx p_n(t)$ if $t \gg 1/(\lambda v_\alpha)$ and $t \gg \hbar/\Gamma$. We will choose the parameters of the model such that $\hbar/\Gamma \gg 1/(\lambda v_\alpha)$. Let us add that Migdal simply calculated $p_n^{\mathrm{I}}(t)$ rather than $P_{\mathrm{inz}}^{\mathrm{I}}(t)$ [1]. This is because he was only interested in the ionization probability in the limit of $t \to \infty$.

We solve the time-dependent Schrödinger equation (2.8) numerically by means of algorithms described in [11–14], and use the 'exact' solution to calculate the transition probabilities. It is useful to compare this exact calculation with perturbation theory. In first order with respect to g we obtain

$$p_n^{\mathrm{pt}}(t) = \left(\frac{g}{\hbar}\right)^2 \left| \int_0^t \mathrm{d}t' \mathrm{e}^{\mathrm{i}(\epsilon_n - \epsilon_1)t'/\hbar} \left[\int_0^\infty \mathrm{d}x_{\mathrm{e}}\, \chi_n^*(x_{\mathrm{e}}) \delta(x_{\mathrm{e}} - v_\alpha t) \chi_1(x_{\mathrm{e}}) \right] \right|^2 \tag{2.14}$$

where $n \neq 1$. Then $P_{n\neq 1}^{\mathrm{I,pt}}(t)$ is given by (2.12) in which p_n is replaced by p_n^{pt}. $p_1(t)$ can be determined by using (2.11).

Let us turn to model II, which we define by means of the Hamiltonian

$$H_{\mathrm{II}} = H_{\mathrm{e}} + H_\alpha + V(x_{\mathrm{e}}, x_\alpha) \tag{2.15}$$

where

$$H_\alpha = \frac{{p_\alpha}^2}{2m_\alpha} + U_\alpha(x_\alpha). \tag{2.16}$$

U_α represents the interaction between the α particle and the daughter nucleus. It consists of a repulsive potential barrier that surrounds an attractive potential. For simplicity we assume that U_α vanishes beyond a certain distance, which is not much larger than the nuclear radius. Unlike model I, model II deals with a two-particle system of the electron and α particle (in the presence of the fixed daughter nucleus). The two-body wavefunction $\Psi(x_{\mathrm{e}}, x_\alpha, t)$ is determined by solving

$$\left(\mathrm{i}\hbar\frac{\partial}{\partial t} - H_{\mathrm{II}}\right)\Psi(x_{\mathrm{e}}, x_\alpha, t) = 0. \tag{2.17}$$

This equation as such is difficult to solve numerically because there are two very different distance scales involved, i.e. atomic and nuclear distances.

Our strategy for finding a solution to (2.17) is to solve it in two steps. In the first step we solve

$$\left(\mathrm{i}\hbar\frac{\partial}{\partial t} - H_\alpha\right)\psi_\alpha(x_\alpha, t) = 0. \tag{2.18}$$

Equation (2.18) determines, in the absence of the electron, how the wavefunction of the emitted α particle is propagated. Solving (2.18) itself is already a nontrivial problem, which we have recently discussed in considerable detail [15, 16]. We assume that the decay process is a very slow one and that it obeys the exponential decay law. We have found that ψ_α in such a case can be reduced to a simple form in a very good approximation. As far as ψ_α well outside the nucleus is concerned, the details of U_α are unimportant. The approximate expression for ψ_α is [15]

$$\psi_\alpha(x_\alpha, t) = -\sqrt{\rho_\alpha(x_\alpha, t)}\exp\left\{-\frac{\mathrm{i}}{\hbar}\left[E_\alpha - \frac{1}{2m_\alpha}\left(\frac{\Gamma}{2v_\alpha}\right)^2\right]t + \mathrm{i}k_\alpha x_\alpha\right\} \quad (2.19)$$

$$\rho_\alpha(x_\alpha, t) = \mathrm{e}^{-\Gamma t/\hbar}\rho_\rho(x_\alpha, 0) + \frac{\Gamma}{\hbar v_\alpha}\exp\left[-\frac{\Gamma}{\hbar}\left(t - \frac{x_\alpha}{v_\alpha}\right)\right]\theta\left(t - \frac{x_\alpha}{v_\alpha}\right) \quad (2.20)$$

where $E_\alpha = m_\alpha v_\alpha^2/2$ is the energy of the α particle, Γ is its width and $k_\alpha = m_\alpha v_\alpha/\hbar$. ρ_α is the probability density of the α particle; $\theta(x) = 1(0)$ for $x > 0$ ($x < 0$). $\rho_\alpha(x_\alpha, 0)$ is the initial density distribution, which is confined within the nucleus. The term $\mathrm{e}^{-\Gamma t/\hbar}\rho_\alpha(x_\alpha, 0)$ of (2.20) refers to the α particle still remaining in the nucleus. It is understood that $\int_0^\infty \mathrm{d}x\, \rho_\alpha(x, 0) = 1$. Then it follows that $\int_0^\infty \mathrm{d}x\, \rho_\alpha(x, t) = 1$ for any $t > 0$. On the atomic scale the nuclear radius is practically zero. In this sense $\rho(x_\alpha, 0)$ can be taken as $\delta(x_\alpha)$ with the understanding that $\int \mathrm{d}x\, \delta(x) = 1$. Actually this δ-function term of $\rho_\alpha(x_\alpha, t)$ has no effect on the electron because, as we have already pointed out for model I, we assume that the electron wavefunction vanishes at $x = 0$. Its effects will be included in the variants of the models which we examine in section 4.

Before proceeding to the next step of solving (2.17) let us examine the structure of $\psi_\alpha(x_\alpha, t)$ of (2.19) in some detail. It has a 'wavefront' at $x_\alpha = v_\alpha t$. The amplitude of $\psi_\alpha(x_\alpha, t)$ at the wavefront is $\sqrt{\Gamma/(\hbar v_\alpha)}$, which is very small in the slow-decay situations that we consider. The amplitude at the typical atomic distance of $x_\alpha = \lambda^{-1}$ is given by

$$\rho^{1/2}(\lambda^{-1}, t) = \sqrt{\frac{\Gamma}{\hbar v_\alpha}}\exp\left[-\frac{\Gamma}{2\hbar}\left(t - \frac{1}{\lambda v_\alpha}\right)\right]. \quad (2.21)$$

After the wavefront passes this position of $x_\alpha = \lambda^{-1}$ the amplitude steadily decreases from its maximum value of $\sqrt{\Gamma/(\hbar v_\alpha)}$. The expectation value of x_α with respect to $\psi_\alpha(x_\alpha, t)$ is given by

$$\langle\psi_\alpha|x_\alpha|\psi_\alpha\rangle = \int_0^\infty \mathrm{d}x_\alpha\, \rho(x_\alpha, t)x_\alpha = v_\alpha t - \frac{\hbar v_\alpha}{\Gamma}(1 - \mathrm{e}^{-\Gamma t/\hbar}). \quad (2.22)$$

Its speed is given by

$$\frac{\mathrm{d}}{\mathrm{d}t}\langle\psi_\alpha|x_\alpha|\psi_\alpha\rangle = v_\alpha(1 - \mathrm{e}^{-\Gamma t/\hbar}). \quad (2.23)$$

When $\Gamma t/\hbar \ll 1$, we obtain

$$\frac{1}{v_\alpha}\frac{\mathrm{d}}{\mathrm{d}t}\langle\psi_\alpha|x_\alpha|\psi_\alpha\rangle \to \frac{\Gamma t}{\hbar} \ll 1. \quad (2.24)$$

Although the wavefront moves at speed v_α, the average position of the α particle moves at a much smaller speed in the early stage of the decay process. This is because the bulk of the wavefunction is still within the nucleus. As t becomes greater than $\Gamma/\hbar$ the average velocity approaches v_α. By that time however the amplitude of (2.21) has become very small, and most of the wavefunction has escaped from the atomic region.

In the second step of solving (2.17) we write $\Psi(x_\mathrm{e}, x_\alpha, t)$ as

$$\Psi(x_\mathrm{e}, x_\alpha, t) = \psi_\alpha(x_\alpha, t)\psi(x_\mathrm{e}, x_\alpha, t). \quad (2.25)$$

By putting this expression into (2.17) we obtain

$$\psi_\alpha(x_\alpha,t)\left(\mathrm{i}\hbar\frac{\partial}{\partial t}-H_\mathrm{e}-V\right)\psi(x_\mathrm{e},x_\alpha,t)+\frac{\hbar^2}{2m_\alpha}\left(\psi_\alpha\frac{\partial}{\partial x_\alpha}+2\frac{\partial\psi_\alpha}{\partial x_\alpha}\right)\frac{\partial\psi(x_\mathrm{e},x_\alpha,t)}{\partial x_\alpha}=0. \tag{2.26}$$

We will use the approximate ψ_α of (2.19) throughout the following calculations. We then obtain

$$2\frac{\partial\psi_\alpha}{\partial x_\alpha}=F(x_\alpha,t)\psi_\alpha \qquad \text{where} \quad F(x_\alpha,t)\equiv 2\mathrm{i}k_\alpha+\frac{1}{\rho_\alpha}\frac{\partial\rho_\alpha}{\partial x_\alpha}. \tag{2.27}$$

Then (2.26) can be reduced to

$$\left[\mathrm{i}\hbar\frac{\partial}{\partial t}-H_\mathrm{e}-V+\frac{\hbar^2}{2m_\alpha}\left(\frac{\partial^2}{\partial x_\alpha^2}+F\frac{\partial}{\partial x_\alpha}\right)\right]\psi(x_\mathrm{e},x_\alpha,t)=0. \tag{2.28}$$

We are interested in solutions of (2.26) and/or (2.28) with the initial condition

$$\psi(x_\mathrm{e},x_\alpha,0)=\chi_1(x_\mathrm{e}). \tag{2.29}$$

If we take the θ function of ρ_α literally, the term $(1/\rho_\alpha)\partial\rho_\alpha/\partial x_\alpha$ of (2.27) is ambiguous. In the actual calculations, therefore, we replace $\theta(x)$ with

$$f(x)=\frac{1}{1+\mathrm{e}^{-\gamma x}} \tag{2.30}$$

where $\gamma>0$ is a constant. It is understood that $1/\gamma$ is of the order of the nuclear size, much smaller than the atomic radius. As long as $1/\gamma$ is very small on the atomic scale, the ionization process is insensitive to γ. In numerical calculations we use $1/\gamma=\Delta x$ where Δx is the mesh that we specify in the next section. Note that $f^{-1}(x)\,\mathrm{d}f(x)/\mathrm{d}x=\gamma f(-x)$. Hence we use the following expression:

$$F(x_\alpha,t)=2\mathrm{i}k_\alpha+\frac{\Gamma}{\hbar v_\alpha}-\frac{\gamma}{v_\alpha}f\left(-t+\frac{x_\alpha}{v_\alpha}\right) \tag{2.31}$$

in (2.28).

Equations (2.26) and (2.28) are still not easy to solve because there are two spatial coordinates involved. Therefore we simplify the model in two ways, which we will refer to as models IIa and IIb. In model IIa we assume that $\psi(x_\mathrm{e},x_\alpha,t)$ is independent of x_α. This may seem like a drastic assumption but we will see that this is actually a reasonably good approximation, at least for the case where the electron is not too tightly bound in the atom. Since $\partial\psi(x_\mathrm{e},x_\alpha,t)/\partial x_\alpha=0$, equation (2.26) becomes much simpler. By multiplying it by ψ_α^* and integrating with respect to x_α we obtain

$$\left[\mathrm{i}\hbar\frac{\partial}{\partial t}-H_\mathrm{e}-g\rho_\alpha(x_\mathrm{e},t)\right]\psi(x_\mathrm{e},t)=0. \tag{2.32}$$

This is simply the Hartree equation for the electron. m_α does not appear in this equation. All the information on the nuclear α decay is contained in $\rho_\alpha(x_\mathrm{e},t)$. If we replace $\rho_\alpha(x_\mathrm{e},t)$ with $\delta(x_\mathrm{e}-v_\alpha t)$, (2.32) is reduced to (2.8) of model I with $V(x_\mathrm{e},x_\alpha)=-g\delta(x_\mathrm{e}-v_\alpha t)$, but this $\delta(x_\mathrm{e}-v_\alpha t)$ is very different from $\rho_\alpha(x_\alpha,t)$ of (2.20). Recall also (2.23). Equations (2.8) and (2.32) are bound to lead to very different results.

The atomic transition probabilities can be calculated by

$$P_n^{\mathrm{IIa}}(t)=\left|\int_0^\infty \mathrm{d}x_\mathrm{e}\,\chi_n^*(x_\mathrm{e})\psi(x_\mathrm{e},t)\right|^2. \tag{2.33}$$

These probabilities add up as

$$\sum_{n=1,3} P_n^{\mathrm{IIa}}(t) + P_{\mathrm{inz}}^{\mathrm{IIa}}(t) = 1 \qquad \text{where} \quad P_{\mathrm{inz}}^{\mathrm{IIa}}(t) = \int_0^\infty \mathrm{d}\epsilon\, P_\epsilon^{\mathrm{IIa}}(t). \tag{2.34}$$

If we use first-order perturbation theory we obtain

$$P_n^{\mathrm{IIa,pt}}(t) = \left(\frac{g}{\hbar}\right)^2 \left| \int_0^t \mathrm{d}t' \mathrm{e}^{\mathrm{i}(\epsilon_n-\epsilon_1)t'/\hbar} \left[\int_0^\infty \mathrm{d}x_\mathrm{e}\, \chi_n^*(x_\mathrm{e}) \rho_\alpha(x_\mathrm{e}, t') \chi_1(x_\mathrm{e}) \right] \right|^2. \tag{2.35}$$

These are to be compared with $P_n^{\mathrm{I}}(t)$ of (2.12).

In model IIa, we have assumed that ψ is independent of x_α. Because of this assumption some details of the correlation between the electron and the α particle are ignored. The phase of $\psi_\alpha(x_\alpha, t)$ does not play any role in model IIa. In model IIb we take account of the x_α dependence of $\psi(x_\mathrm{e}, x_\alpha, t)$. On the other hand, however, we assume that the electron–α interaction is weak and we can treat it by first-order perturbation theory. We expand $\psi(x_\mathrm{e}, x_\alpha, t)$ in terms of the stationary wavefunctions of the electron,

$$\psi(x_\mathrm{e}, x_\alpha, t) = \sum_{n=1,3} C_n(x_\alpha, t)\chi_n(x_\mathrm{e})\mathrm{e}^{-\mathrm{i}\epsilon_n t/\hbar} + \int_0^\infty \mathrm{d}\epsilon\, C_\epsilon(x_\alpha, t)\chi_\epsilon(x_\mathrm{e})\mathrm{e}^{-\mathrm{i}\epsilon t/\hbar}. \tag{2.36}$$

It is understood that

$$C_1(x_\alpha, 0) = 1 \qquad C_3(x_\alpha, 0) = 0 \qquad C_\epsilon(x_\alpha, 0) = 0. \tag{2.37}$$

Expanding the C in powers of g and retaining the terms that are of first order in g, we obtain

$$\left[\mathrm{i}\hbar\frac{\partial}{\partial t} + \frac{\hbar^2}{2m_\alpha}\left(\frac{\partial^2}{\partial x_\alpha^2} + F\frac{\partial}{\partial x_\alpha}\right)\right] C_n(x_\alpha, t) = -g\,\chi_n^*(x_\alpha)\chi_1(x_\alpha)\mathrm{e}^{\mathrm{i}(\epsilon_n-\epsilon_1)t/\hbar} \tag{2.38}$$

where $n \neq 1$ and a similar equation for $C_\epsilon(x_\alpha, t)$.

The system starts with the electron in state 1. The probability for finding the electron in state n at time t is determined by the overlap of two wavefunctions. One of them is $\psi_\alpha(x_\alpha, t)$ multiplied by $\psi(x_\mathrm{e}, x_\alpha, t)$ of (2.36) and the other is $\psi_\alpha(x_\alpha, t)\chi_n(x_\mathrm{e})\mathrm{e}^{-\mathrm{i}\epsilon_n t/\hbar}$. The transition probability into the electron state n is given by

$$P_n^{\mathrm{IIb}}(t) = \left| \int_0^\infty \mathrm{d}x_\alpha\, \rho_\alpha(x_\alpha, t) C_n(x_\alpha, t) \right|^2. \tag{2.39}$$

We compare this with $P_n^{\mathrm{I}}(t)$ and $P_n^{\mathrm{IIa}}(t)$ obtained earlier.

3. Calculations and results

Let us begin with determining the parameters in the models. In this and the next sections we use natural units such that $c = \hbar = 1$. For the energy and mass we use MeV or eV. For distance x we use units of MeV^{-1} or Å ($=10^{-8}$ cm^{-1}). For t we use MeV^{-1} or s. In this system of units, 1 MeV^{-1} and 197.3 fm $= 1.973 \times 10^{-3}$ Å and $(1.973/2.998) \times 10^{-21}$ s are interchangeable. The speed is dimensionless.

For the masses we use the following approximate values:

$$m_\mathrm{e} = 0.5\ \mathrm{MeV} \qquad m_\alpha = 4000\ \mathrm{MeV}. \tag{3.1}$$

For the potential of $U_\mathrm{e}(x_\mathrm{e})$ of (2.3) we take $N = 4$. Then there are two bound states, with $n = 1$ and 3. For the energy of the ground state ϵ_1 we consider two cases, loose binding (LB) and tight binding (TB). The energy of the excited state is $\epsilon_3 = (\frac{4}{9})\epsilon_1$. The parameters are summarized in table 1. The rationale for these choices is given after we have discussed the

Table 1. 'Atomic' parameters for the LB and the TB cases.

Case	ϵ_1 (eV)	ϵ_3 (eV)	$1/\lambda$	v_e
LB	−20	−8.89	671.0 MeV^{-1} = 1.32 Å	0.013
TB	−2000	−889	67.1 MeV^{-1} = 0.132 Å	0.13

properties of the α particle. The strength parameter g of the electron–α interaction V is chosen so that the binding energy of the electron due to V alone is 25 eV, i.e.

$$\tfrac{1}{2}g^2 m_e = 25 \text{ eV} \qquad g = 0.01. \tag{3.2}$$

The α-decay process is characterized by the energy of the α particle $E_\alpha = m_\alpha v_\alpha^2/2$ and the energy width Γ. The latter is related to the decay half-life by $\tau_{1/2} = (\ln 2)/\Gamma$. In order to obtain realistic values of these quantities, let us consider Po^{212} as the parent nucleus. Its decay rate is the fastest among the usually listed α-decay examples: see, e.g., [17]. In this case $E_\alpha = 8.95$ MeV, $\Gamma = 1.52 \times 10^{-9}$ eV $= 2.31 \times 10^6$ s^{-1} and $\tau_{1/2} = 3.0 \times 10^{-7}$ s.

In our models we set E_α as

$$E_\alpha = 5 \text{ MeV} \qquad v_\alpha = 0.05. \tag{3.3}$$

For the energy width Γ we take

$$\Gamma = 2 \text{ eV}. \tag{3.4}$$

Then the decay half-life becomes

$$\tau_{1/2} \approx 0.347 \text{ eV}^{-1} \approx 2.3 \times 10^{-16} \text{ s}. \tag{3.5}$$

This half-life is unrealistically short. The reason for assuming such a short half-life is the following. When solving the time-dependent Schrödinger equation of the models, in order to be able to see anything interesting, we have to solve it at least up to a value of t comparable to $\tau_{1/2}$. This is difficult if $\tau_{1/2}$ is very large. For the purpose of simulation, $\tau_{1/2}$ of (3.5) is large enough because the time for the α particle to traverse the model atom is much shorter than the decay half-life. Recall that the radius of the model atom is of the order of $1/\lambda$. The α particle traverses this distance in the time interval of $1/(\lambda v_\alpha)$. If we take $1/\lambda = 1.32$ Å, then we find, with $v_\alpha = 0.05$, $1/(\lambda v_\alpha) \approx 8.8 \times 10^{-18}$ s, which is much smaller than the $\tau_{1/2}$ of (3.5).

Let us estimate the speed of the electron in the initial bound state. The expectation value of the kinetic energy of the electron in state 1 is roughly equal to $-2\epsilon_1$. Hence the average speed of the electron v_e can be estimated by $v_e \approx \sqrt{-2\epsilon_1/m_e}$. This leads to values of v_e in table 1 for the two choices of ϵ_1. These values can be compared with the assumed speed of the α particle, $v_\alpha = 0.05$. The two choices of the value of ϵ_1 in table 1 represent two typical situations in which v_α is greater or smaller than v_e. The binding energy of the K-shell electron can be almost as large as 0.1 MeV. We have chosen values much smaller than this because (2.38) becomes more difficult to solve if $\epsilon_n - \epsilon_1$ is very large.

We solve the time-dependent Schrödinger equations numerically. We do this by discretizing x and t, with $\Delta x = 1\,\text{MeV}^{-1} \approx 2.0 \times 10^{-3}$ Å and $\Delta t = 5\,\text{MeV}^{-1} \approx 3.3 \times 10^{-21}$ s. In integrating the equations, we take $x_{\max} = 7.5 \times 10^4$ MeV^{-1} and $t_{\max} = 5 \times 10^5$ MeV^{-1}. Recall that $\tau_{1/2} \approx 3.47 \times 10^5$ MeV^{-1}. This value of $x_{\max}$ is sufficiently large such that, for the chosen $t_{\max}$, the results are insensitive to $x_{\max}$.

In presenting the results of the calculations, we start with the LB case. Figure 1 shows $|\psi(x_e, t)|$. The major peak near the origin represents the electron in the atom. There are two smaller peaks that are travelling out. The smaller of the two represents the electron bound to the α particle. It moves at speed $v_\alpha = 0.05$. The larger peak travels at speed $2v_\alpha = 0.1$. The

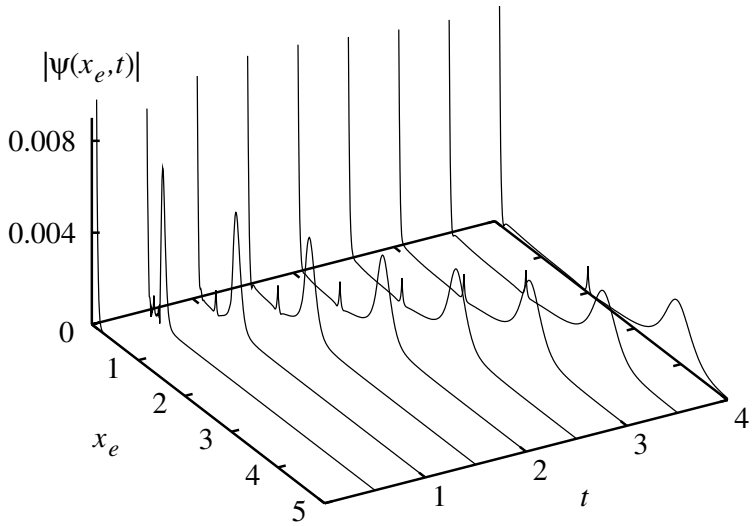

Figure 1. The modulus $|\psi(x_e, t)|$ in units of $\mathrm{MeV}^{1/2}$ of the LB case of model I. Both variables x and t are in units of $\mathrm{MeV}^{-1} \approx 2.0 \times 10^{-3}$ Å $\approx 0.66 \times 10^{-21}$ s. The axes are scaled so that x_e is in units of 10^4 MeV^{-1} and t in units of 10^5 MeV^{-1}.

Table 2. Transition probabilities for a time period equal to the half-life of decaying 'nucleus' for the light-binding case. The first row corresponds to the calculations in this paper; the second row gives the first-order perturbation results for the same quantities.

Calculation	$p_3(\tau_{1/2})$	$P_3^{\mathrm{I}}(\tau_{1/2})$	$P_3^{\mathrm{IIa}}(\tau_{1/2})$
Model	1.08×10^{-4}	7.59×10^{-5}	1.67×10^{-6}
Perturbation	1.28×10^{-4}	8.55×10^{-5}	1.67×10^{-6}

latter represents the electron that has been knocked out by the α particle. This corresponds to the situation in classical mechanics in which a light particle at rest is hit by a heavy particle and obtains a speed twice that of the heavy particle.

In comparing the probabilities obtained in different models we focus on the transition $1 \to 3$. Figure 2 shows $p_3(t)$ and $P_3^{\mathrm{I}}(t)$. Recall that $\tau_{1/2} = 3.47 \times 10^5$ MeV^{-1}. Although we do not show them, $p_3^{\mathrm{pt}}(t)$ and $P_3^{\mathrm{I,pt}}(t)$ are very similar to their counterparts shown in figure 2. These probabilities at $t = \tau_{1/2}$ are listed in table 2. The perturbation theory somewhat overestimates the probabilities. We have also calculated the probability for the electron to remain in the ground state and that for going into continuum states. We have found that (2.11) is very accurately satisfied.

Let us turn to models IIa and IIb. Figure 3 shows $|\psi(x_e, t)|$ of model IIa. This can be compared with figure 1 of model I. Note the difference in the scale. Unlike the case in figure 1, only one travelling peak is noticeable. Its speed is $2 \times v_\alpha = 0.1$. This peak is caused by the sharp wavefront of $\psi_\alpha(x_\alpha, t)$, that travels at speed v_α. This peak is smaller by a factor of 10^{-3} in its height than its counterpart of model I. Figure 4 shows $P_3^{\mathrm{IIa}}(t)$ and $P_{\mathrm{inz}}^{\mathrm{IIa}}(t)$ as functions of t.

At $t = \tau_{1/2}$ we obtain

$$P_3^{\mathrm{IIa}}(\tau_{1/2}) = 1.67 \times 10^{-6} \tag{3.6}$$

$$P_3^{\mathrm{IIa,pt}}(\tau_{1/2}) = 1.67 \times 10^{-6}. \tag{3.7}$$

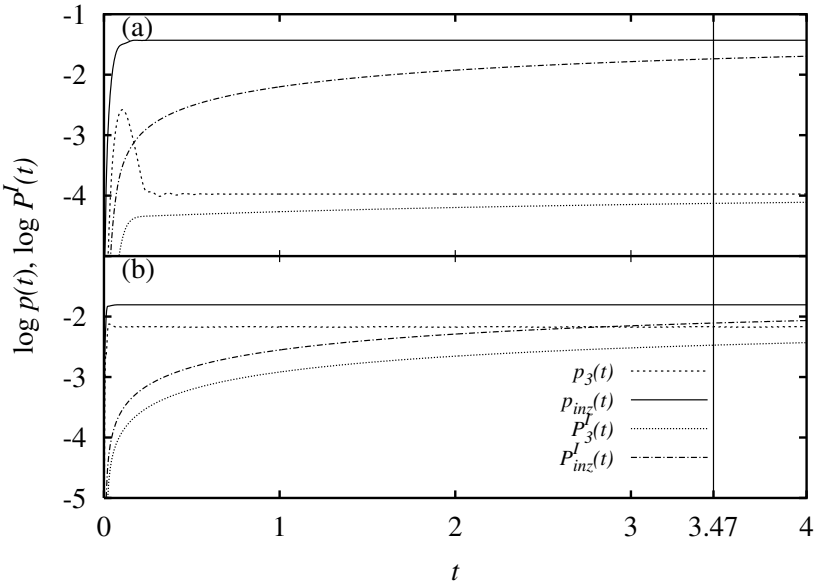

Figure 2. The probabilities $P_3^{\mathrm{I}}(t)$ and $p(t)$ of model I for the LB case in graph (a) and for the TB case in graph (b). The unit for t is the same as in figure 1.

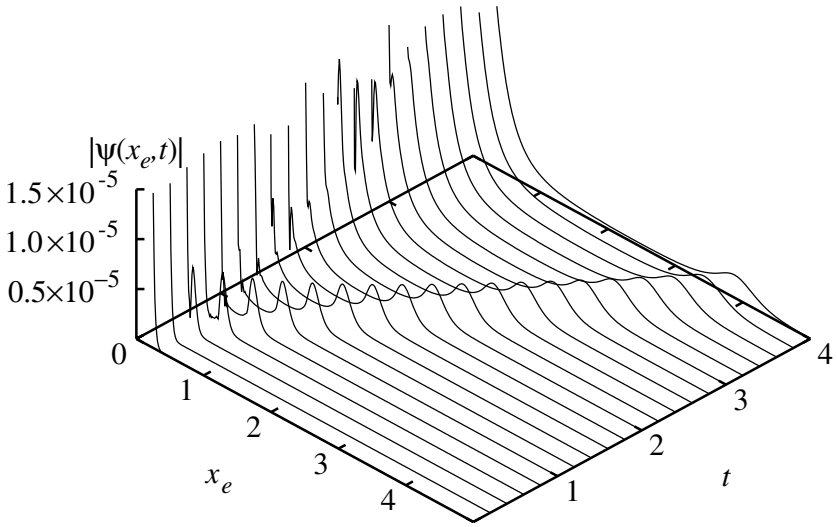

Figure 3. The modulus $|\psi(x_{\mathrm{e}}, t)|$ in units of $\mathrm{MeV}^{1/2}$ of model IIa for the LB case. The units are the same as those of figure 1.

For model IIa the perturbation calculation is very accurate. We have again calculated the probability for the electron remaining in the ground state and that for going into continuum states. We have confirmed that (2.13) is very accurately satisfied.

In model IIb, we found it more difficult to solve (2.36) than (2.8) and (2.32). We encountered an instability when t exceeded 7×10^4 MeV^{-1}. Figure 5 shows $P_3^{\mathrm{IIb}}(t)$ only up to $t = 1 \times 10^4$ MeV^{-1}. The results for $t = 5 \times 10^4$ MeV^{-1} are listed in table 3. The

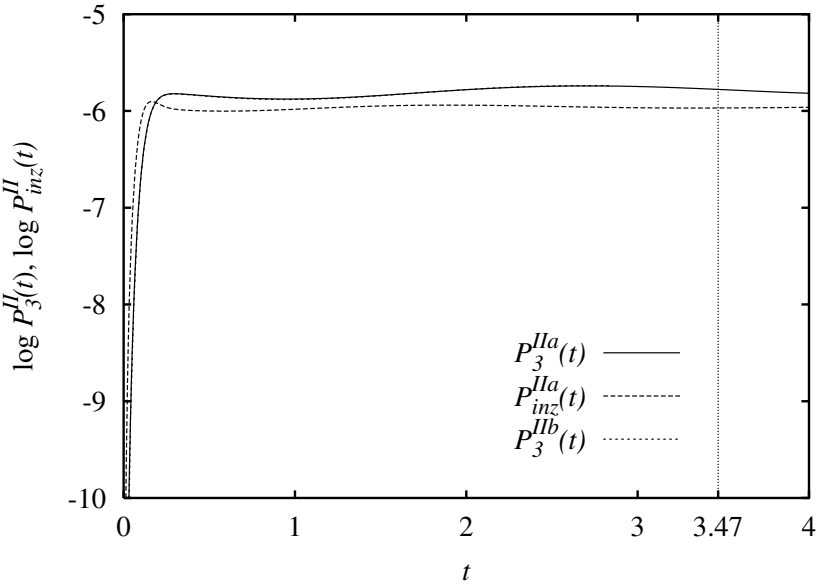

Figure 4. The probabilities $P_3(t)$ for models IIa and IIb and $P_{\rm inz}(t)$ for model IIa for the LB case. Probability $P_3(t)$ is identical for both versions of model II. The units are the same as those of figure 1.

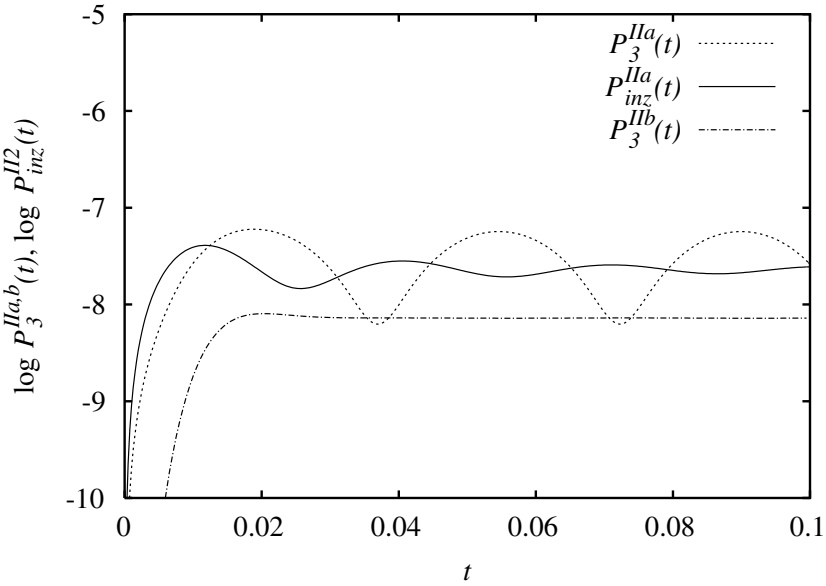

Figure 5. The probabilities $P_3^{\rm IIa}(t)$, $P_{\rm inz}^{\rm IIa}(t)$ and $P_3^{\rm IIb}(t)$ for model II and the TB case. The units are the same as those of figure 1.

probabilities of models IIa and IIb agree very well for the LB case and reasonably well for the TB case, but for both cases they are much smaller than that of model I.

In the TB case we have listed the probabilities at $t = 1 \times 10^4$ MeV^{-1}. $P_3^{\rm IIa}(t)$ actually

Table 3. Comparison of transition probabilities to state $n = 3$ of the three models.

Case	t (MeV^{-1})	$P^I(t)$	$P_3^{\mathrm{IIa}}(t)$	$P_3^{\mathrm{IIb}}(t)$
LB	5×10^4	1.03×10^{-4}	1.43×10^{-6}	1.42×10^{-6}
TB	1×10^4	6.67×10^{-1}	2.61×10^{-8}	7.23×10^{-9}

shows regular fluctuations between approximate minimum and maximum values of 6×10^{-9} and 6×10^{-8} and with a period of about 3.5×10^3 MeV^{-1}. The value given in table 3 is the average taken over several fluctuations. By $t \approx 2000$ MeV^{-1}, the wavefront of the α-particle wavefunction has left the atom. The wavefront is followed by an exponentially decreasing tail. The small fluctuations seen in the transition probability $P_3^{\mathrm{IIa}}(t)$ are probably due to this tail, which causes multiple excitations and deexcitations. $P_3^{\mathrm{IIb}}(t)$ does not show such fluctuations because it has been obtained in a first-order perturbation calculation, which does not take account of the possibility of multiple interaction processes. As compared with the LB case, for the TB case $P_3^{\mathrm{I}}(t)$ is larger, while $P_3^{\mathrm{IIa}}(t)$ and $P_3^{\mathrm{IIb}}(t)$ are smaller. Therefore the gap between models I and II has become much larger.

Let us add that, for the α–electron interaction, we also examined a smeared-out version of the δ-function potential. We used a potential of the Gaussian form and varied its width up to 20 in units of Δx. We confirmed that the results are insensitive to the change of the width.

4. Effects of the change in the nuclear charge

There are two mechanisms that cause electronic transitions: one is the change in the nuclear charge and the other is the interaction between the electron and the travelling α particle. The models we have examined so far do not accommodate the effect of the change in the nuclear charge for the following reasons.

In model I, the α particle is at $x = 0$ at $t = 0$. The charge localized around the origin suddenly disappears when the α particle is emitted. Because of the boundary condition that the electron wavefunctions all vanish at the origin and that the electron–α interaction is a δ function, the electron does not feel this sudden change at the origin. The electron wavefunction at $t = 0$ is $\chi_1(x_\mathrm{e})$, an eigenstate of H_e of (2.2). H_e does not include the interaction due to the α particle.

In model II the probability density for the α particle is given by (2.20). The first term $\mathrm{e}^{-\Gamma t/\hbar}\rho_\alpha(x_\alpha, 0)$ represents the α particle that is still within the nucleus; the latter is taken as a point particle and $\rho_\alpha(x_\alpha, 0)$ is replaced with $\delta(x_\alpha)$. In sharp contrast to model I the charge localized around the origin decreases in time very gradually. The electron however is again insensitive to the charge at the origin for the same reason as we explained in the preceding paragraph.

In this section we propose variants of the two models. Instead of the half-space of $x > 0$ that we considered before, we now consider the entire space of $x > 0$ and $x \leqslant 0$. Then the ground state of the model atom is of even parity and the α particle at the origin has an effect on it. There were two reasons why we did not do so from the beginning. One is that it is somewhat easier to solve the equations of the model if we restrict ourselves to $x > 0$. The other is that we wanted to isolate the effect of the electron–α interaction.

We consider models I and IIa but for the entire space and will refer to these alternative versions as I′ and II′, respectively. We do not consider model IIb because we have seen that the results of models IIa and IIb are very similar. We use the same Hamiltonians as before except for the following two changes. One of the changes is concerned with potential U_e. This time

we take $N = 3$ so that U supports three bound states of $n = 0$, $n = 1$ and $n = 2$. For λ we keep the same value as before. Then the lowest eigenvalue of H_e with the revised U_e, which we denote by ϵ_0, remains the same as before,

$$\epsilon_0 = -\frac{4\lambda^2}{2m_e} = \begin{cases} -20 \text{ eV} & \text{(LB)} \\ -2000 \text{ eV} & \text{(TB).} \end{cases} \tag{4.1}$$

The higher eigenvalues are related to ϵ_0 by $\epsilon_1 = (\frac{4}{9})\epsilon_0$ and $\epsilon_2 = (\frac{1}{9})\epsilon_0$. The Hamiltonian H_e determines the atom after the α particle has been completely removed. For finite t, the atom is subject to the interaction that consists of U_e and the interaction with the α particle.

The other change is for the probability density that appears in model II′. We replace $\rho_\alpha(x_\alpha, t)$ of (2.20) with

$$\rho'_\alpha(x_\alpha, t) = \mathrm{e}^{-\Gamma t/\hbar}\delta(x_\alpha) + \frac{\Gamma}{2\hbar v_\alpha} \exp\left[-\frac{\Gamma}{\hbar}\left(t - \frac{|x_\alpha|}{v_\alpha}\right)\right]\theta\left(t - \frac{|x_\alpha|}{v_\alpha}\right). \tag{4.2}$$

The wavefunction of the α particle propagates out in both the positive and negative x directions. Note, however, that the α particle travels only in one (positive x) direction in model I′. Model II′ has left–right symmetry but the symmetry is broken in model I′.

The time-dependent Schrödinger equation for model I′ is the same as (2.8). The equation for model II′ is (2.32) in which ρ_α is replaced by ρ'_α. There is an important change in the initial condition. In models I and II the electron wavefunction started as $\chi_1(x_e)$; see (2.9) and (2.29). This time the initial electron wavefunction is $\chi'_0(x_e)$, that is, the ground state solution (with $n = 0$) of

$$[H_e - g\delta(x_e) - \epsilon'_n]\chi'_n(x_e) = 0. \tag{4.3}$$

Note that $\epsilon'_n < \epsilon_n$ for $n = 0$ and 2 because of the additional attraction at the origin. The odd-parity state of $n = 1$ is not affected by the δ-function potential at the origin. The δ-function potential makes the derivative of the even-parity wavefunction discontinuous, i.e.

$$\frac{\mathrm{d}\chi'_n}{\mathrm{d}x_e}(0^+) = -gm_e\chi'_n(0) \tag{4.4}$$

for $n = 0, 2$.

Although we only need the solution of $n = 0$ in our actual calculations, let us examine how the energies of the states of $n = 0$ and 2 are affected by the δ-function potential at the origin. In first-order perturbation theory we obtain

$$\epsilon_0^{\mathrm{pt}} = \epsilon_0 - \tfrac{15}{16}g\lambda \qquad \epsilon_2^{\mathrm{pt}} = \epsilon_2 - \tfrac{3}{16}g\lambda. \tag{4.5}$$

We also solve (4.3) numerically to obtain the exact energies. The results are displayed in table 4. The excited state of $n = 1$ is of odd parity and is not affected by the δ-function potential at the origin.

Long after the α particle has escaped from the atom, the electron state becomes a superposition of eigenstates of H_e. We are interested in the transitions to the eigenstates of H_e, which we designate by $n = 0, 1, 2$ and ϵ. The transition probabilities can be calculated in the same manner as for models I and II. Note however from the last line of table 4 that $p_0(0) < 1$ and $p_2(0) \neq 0$. Since the sum of the probabilities must add to unity the $p_\epsilon(0)$ are not all zero either.

In figure 6 we plot the magnitude of the wavefunction $|\psi(x_e, t)|$ for model I′. The initial wavefunction has a discontinuous slope at $x_e = 0$ because of the δ-function component of the atomic potential, but in time the latter moves to the right with the α particle and can be seen as the spike which represents the electron captured by the α particle. The atomic wavefunction reverts to that of the daughter nucleus with a smaller binding energy and hence a more spread

Table 4. Properties of the parent and daughter nuclei for the LB and TB cases when the system extends over the range $-\infty < x < \infty$.

	$\lambda = 1491$ eV (LB)			$\lambda = 14\,910$ eV (TB)		
	$n = 0$	$n = 1$	$n = 2$	$n = 0$	$n = 1$	$n = 2$
ϵ_n (eV)	−20.0	−8.89	−2.22	−2000	−889	−222
ϵ'_n (eV)	−50.7	−8.89	−5.10	−2150	−889	−251
$\epsilon_n^{\rm pt}$ (eV)	−34.0	−8.89	−5.02	−2140	−889	−250
$p_n(0)$	0.7633	0.0000	0.0612	0.9972	0.0000	0.0012

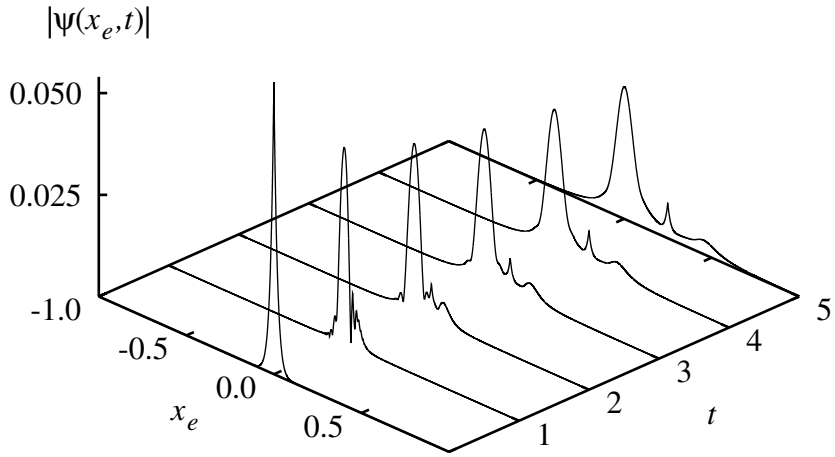

Figure 6. The modulus $|\psi(x_{\rm e}, t)|$ in units of $\mathrm{MeV}^{1/2}$ of the LB case of model I′. The axes are scaled so that $x_{\rm e}$ is in units of 10^4 MeV^{-1} and t is in units of 10^4 MeV^{-1}.

out wavefunction. As is the case with model I there is a peak in the wavefunction that travels with twice the speed of the α particle. Clearly the initial symmetry of the wavefunction is broken since the α particle has a constant velocity to the right. For model II′ the wave function remains symmetric and has a travelling peak in both directions, compared to the wavefunction shown in figure 3, which has a peak travelling to the right only.

In figure 7 we show graphs of the logarithm of the transition probabilities $p(t)$ as defined in (2.10) for models I′ and II′. The plots show that the more quantum mechanical model yields results that are several orders of magnitude smaller than the model with the classical trajectory of the α particle. We have not shown the decay-rate-averaged transition probabilities (2.12) for model I′, since at large times these probabilities approach $p(t)$. Thus the curves $P^{\rm I'}(t)$ of model I′ would rise more slowly but have the same asymptote as $p^{\rm I'}(t)$. Regarding the transition to state 1, there is a distinct difference between the predictions of models I′ and II′. Note that $p_1^{\rm II'}(t) = 0$. The transition to state 1 is allowed in model I′ but not in model II′. In the latter, parity is conserved. Note also that $P_2^{\rm I'}(t) \gg P_2^{\rm II'}(t)$.

The ionization process in model I′ consists of two parts. First there is a sudden change of the nuclear charge, which can be treated by the sudden approximation, and which causes transitions to excited states of the daughter atom. Secondly the motion or field that the α particle produces results in further transitions to excited levels. In table 5 we show transition probabilities at $t = 0$ and $t = 5 \times 10^4$ MeV^{-1}. The sudden approximation gives a large contribution to the transition probabilities in the case of model I′ and another significant

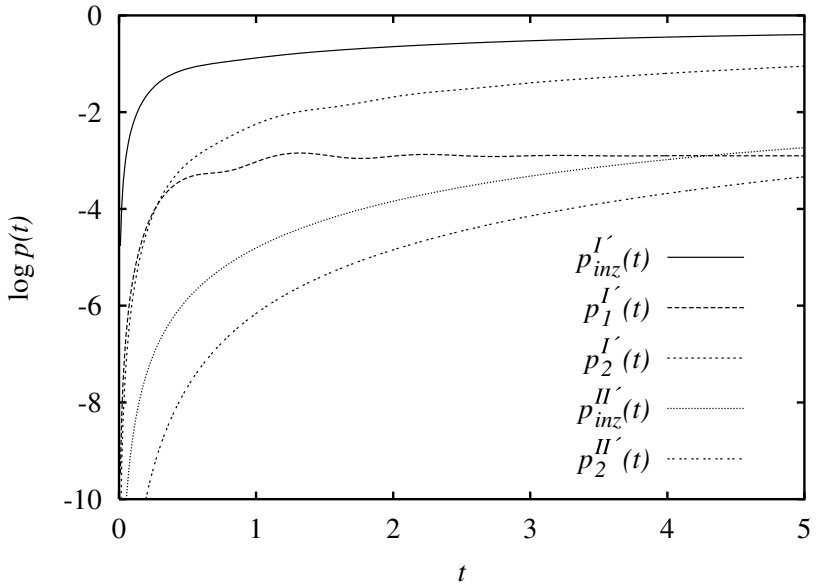

Figure 7. Comparison of the logarithm of the transition probabilities $p(t)$ for models I′ and II′ in the LB case. The horizontal axis is scaled so that t is in units of 10^4 MeV^{-1}.

Table 5. Sudden and long-time transition probabilities for the LB case.

Model	t (MeV^{-1})	$p_0(t)$	$p_1(t)$	$p_2(t)$	$p_{\mathrm{inz}}(t) = \int_0^\infty \mathrm{d}\epsilon\, p_\epsilon(t)$
	0	0.7633	0.0000	0.0612	0.1755
I′	5×10^4	0.5078	0.0013	0.0890	0.4019
II′	5×10^4	0.9977	0.0000	0.0005	0.0018

contribution arises from the changing field due to the travelling α particle. In model II′ the process seems adiabatic. The nuclear charge and the field that the electron experiences changes slowly, so that the system goes primarily from the ground state of the parent atom to that of the daughter atom with small ionization and excitation probabilities.

5. Summary and discussion

In order to gain insight into the mechanism of atomic ionization caused by the nuclear α decay, we examined a system that consists of a daughter nucleus, an α particle and an electron. The nucleus is fixed at the origin. For this system we considered schematic models of two types: type I with variants labelled I and I′, and type II with variants II and II′. The two types differ in the way the α particle is treated. In the models of type I the α particle is treated as a classical point particle. This simulates Migdal's approach. The models of type II treat the α particle quantum mechanically. It is represented by a wave that slowly leaks out from the nucleus.

Models I and I′ differ in the treatment of the change in the nuclear charge, but we found that this difference is of minor importance. Models II and II′ differ in the same way. The crux of the problem is that the ionization probability differs by a large factor for the two types of model; that is, it depends on whether the α particle is treated as a classical particle or as a quantum mechanical wave.

In models I and I′, we treated the effects of the α decay on the atom in two ways, one exactly and the other by first-order perturbation theory. We confirmed that first-order perturbation theory works satisfactorily. In models of type II, unlike the models of type I, it is difficult to perform exact calculations. We therefore treated the effects due to the α decay by first-order perturbation theory. Depending on the treatment of the electron–α correlation, we have two versions of model II, referred to as IIa and IIb, but the difference between these two versions turns out not to be very important. See table 3 and figures 4 and 5.

Although there is room for improvement in the calculations of the models of type II, it is clear that these models make predictions of the ionization or excitation probabilities which are significantly smaller than those of the models of type I. For computational convenience we assumed much larger than realistic values for the α-decay width Γ. If we consider realistic values of Γ, the difference in the results of the two types of model would be much larger. As far as we know time-dependent quantum mechanical calculations of this nature for the ionization problem have not been performed before. The calculations of models of type II confirm the notion that in decaying systems with long half-lives the change in the (electric) field experienced by the electrons is so slow that the excitation process is nearly adiabatic. Thus the conclusion to be drawn from this analysis is the paradoxical situation that the fully quantum mechanical calculations with the models of type II give results which do not agree with those of models of type I. However, the models of type I, which are hybrids of quantum and classical mechanics, lead to reasonable agreement with experiment.

It is appropriate to point out that an earlier calculation [18] obtained consistency between results of a semi-classical and a quantum calculation of the atomic ionization due to α decay. (See also [19].) Although in that calculation the α particle is treated quantum mechanically, it is not done in a fully time-dependent manner. The decay problem is treated as that of a quasi-stationary state with complex energy. This implicitly assumes that the nucleus is a constant source of α particles (which is unrealistic). It is interesting that such a treatment leads to results which are approximately equal to those of Migdal. It seems imperative that the time-dependent quantum formalism and its application be examined carefully in view of the results that we have obtained in this paper. This may lead to the discovery of unwarranted assumptions either of a calculational nature or of a more fundamental character.

Finally let us mention another problem which is closely related to the subject of this paper. This is bremsstrahlung in α decay. Triggered by recent experiments [20, 21], there has been a surge of interest in this topic. A few theoretical papers have appeared but let us quote only the very recent one [22], through which one can trace earlier references. We are particularly interested in the time-dependent approach to the bremsstrahlung process of Bertulani *et al* [22]. In the earlier references on this topic, a stationary or quasi-stationary approach is taken. Bertulani *et al* solved the time-dependent Schrödinger equation for α decay. By using the thus-obtained wavefunction of the α particle, they calculated the average radial momentum $p_r(t)$, which corresponds to our $m(\mathrm{d}/\mathrm{d}t)\langle\psi_\alpha|x|\psi_\alpha\rangle$. They found this $p_r(t)$ to be much smaller than its classical counterpart. This is consistent with what we pointed out below (2.23). By using $p_r(t)$ as the momentum of a classical particle of charge 2, they calculated the bremsstrahlung probability. The probability so obtained is naturally much smaller than the probability (except for a photon-energy range around 8 MeV) that follows from a classical approach with the classical counterpart of momentum $p_r(t)$. The results of Bertulani *et al* as such cannot be compared directly with experiments because the situation that they chose (for computational convenience) does not exactly correspond to those of experiments [20, 21]. If their calculation were performed for experimental situations (which is quite prohibitive as they pointed out), it would probably result in an emission probability significantly smaller than the experimental value. There is an obvious similarity between the results of Bertulani *et al* and ours.

Acknowledgments

We would like to thank Dr V G Zelevinsky for helpful communication regarding [22] and Dr C V K Baba for calling our attention to some literature on related problems. This work was supported by the Natural Sciences and Engineering Research Council of Canada.

Appendix A. Pöschl–Teller potential

In this appendix we give wavefunctions for the relevant eigenstates of H_e of (2.2) with the Pöschl–Teller potential of (2.3). We suppress subscript e of x_e. We normalize the wavefunctions such that

$$\int_0^\infty \mathrm{d}x\ \chi_n^*(x)\chi_m(x) = \delta_{nm} \qquad \int_0^\infty \mathrm{d}x\ \chi_\epsilon^*(x)\chi_{\epsilon'}(x) = \delta(\epsilon - \epsilon'). \tag{A.1}$$

$\chi_n(x)$ and $\chi_\epsilon(x)$ are orthogonal.

For models I, IIa and IIb, we take $N = 4$. We consider only $x > 0$ and require that the wavefunctions vanish at $x = 0$. Then there are two bound states with $n = 1$ and 3. Their eigenvalues are determined by (2.5). Their wavefunctions are given by

$$\chi_1(x) = \sqrt{105\lambda/8}\sinh\lambda x\cosh^{-4}\lambda x \tag{A.2}$$

$$\chi_3(x) = \sqrt{5\lambda/8}(3 - 4\sinh^2\lambda x)\sinh\lambda x\cosh^{-4}\lambda x. \tag{A.3}$$

The wavefunction of the scattering state of energy $\epsilon = (\hbar k)^2/(2m_e)$ is given by

$$\chi_\epsilon(x) = \sqrt{\frac{2m_e}{\pi\hbar^2 k}}\sin[kx + \delta_k(x)] \tag{A.4}$$

where

$$\tan\delta_k(x) = \frac{5\lambda k[(11\lambda^2 + 2k^2) - 21\lambda^2\tanh^2\lambda x]\tanh\lambda x}{(\lambda^2 + k^2)(9\lambda^2 + k^2) - 45\lambda^2(2\lambda^2 + k^2)\tanh^2\lambda x + 105\lambda^4\tanh^4\lambda x}. \tag{A.5}$$

In models I′ and II′ examined in section 4, we take $N = 3$. We consider the entire x space. The wavefunctions are normalized over $-\infty < x < \infty$. There are three bound states with $n = 0,\ 1$ and 2. Their wavefunctions are given by

$$\chi_0(x) = \left(\sqrt{15\lambda}/4\right)\cosh^{-3}\lambda x, \tag{A.6}$$

$$\chi_1(x) = \left(\sqrt{15\lambda}/2\right)\sinh\lambda x\cosh^{-3}\lambda x, \tag{A.7}$$

$$\chi_2(x) = \left(\sqrt{3\lambda}/4\right)(5 - 4\cosh^2\lambda x)\cosh^{-3}\lambda x. \tag{A.8}$$

This $\chi_1(x)$ is different from that of (A.2) because the value of N of the potential is different. Since we do not calculate the probability of transition into scattering states for these models, we do not give expressions of the scattering wavefunctions.

Appendix B. Atomic ionization caused by a bombarding α particle

Consider an atom in its ground state, which is bombarded by an α particle. The atom may be excited or ionized. Let us simulate this process by means of a simple one-dimensional model. We consider the entire x space as we did in section 4. The model atom, which is fixed at the origin, can take only two states, $|1\rangle$ and $|2\rangle$. In this model, which is much simpler than those we used in the main text, we do not explicitly see the electron. The particle that we refer to in the following simulates the α particle. We suppress subscript α. The atom interacts with the

particle through potential $V(x)$ where x is the coordinate of the particle. The atom is initially in the ground state $|1\rangle$. We examine the probability of finding the atom in the excited state $|2\rangle$ after the collision.

We consider two models, A and B. In model A we treat the particle as a classical point particle travelling with a constant speed v. In model B the incident particle is represented by a wavepacket. Its centre starts with speed v. Models A and B can be compared with models of types I and II, respectively, of the main text the Hamiltonian of the model atom by itself is

$$H_0 = \sum_{n=1}^{2} \epsilon_n |n\rangle\langle n|. \tag{B.1}$$

For the particle-plus-atom system of model A we assume the Hamiltonian

$$H_{\mathrm{A}} = H_0 + V(vt)(|1\rangle\langle 2| + |2\rangle\langle 1|). \tag{B.2}$$

The particle starts at $x_0 < 0$ and moves with constant speed $v > 0$. It passes the centre of the atom at $t = 0$. For the particle–atom interaction potential we assume

$$V(x) = -\frac{g\lambda}{\sqrt{\pi}} \mathrm{e}^{-(\lambda x)^2}. \tag{B.3}$$

It is understood that $V(x_0)$ is negligible. We represent the wavefunction of the two-level atom by

$$\Psi_{\mathrm{A}} = \sum_{n=1}^{2} c_n(t)|n\rangle, \tag{B.4}$$

and solve the time-dependent Schrödinger equation $\mathrm{i}\hbar\partial\Psi_{\mathrm{A}}/\partial t = H_{\mathrm{A}}\Psi_{\mathrm{A}}$ to obtain the coefficients $c_n(t)$.

In model B we assume the Hamiltonian

$$H_{\mathrm{B}} = -\frac{\hbar^2}{2m}\frac{\partial^2}{\partial x^2}\sum_{n=1}^{2}|n\rangle\langle n| + H_{\mathrm{e}} + V(x)(|1\rangle\langle 2| + |2\rangle\langle 1|). \tag{B.5}$$

We write the wavefunction of the particle–atom system as

$$\Psi_{\mathrm{B}} = \sum_{n=1}^{2} \psi_n(x,t)|n\rangle. \tag{B.6}$$

We solve the time-dependent Schrödinger equation of model B with the initial condition for the wavefunction,

$$\psi_1(x,0) = \left(\frac{1}{2\pi {w_0}^2}\right)^{1/4} \exp\left[-\left(\frac{x-x_0}{2w_0}\right)^2 + \frac{\mathrm{i}mv(x-x_0)}{\hbar}\right] \tag{B.7}$$
$$\psi_2(x,0) = 0.$$

$\psi_1(x,0)$ represents a Gaussian wavepacket with its centre at $x = x_0$. The width of the wavepacket is characterized by w_0. The phase factor $\exp[\mathrm{i}mv(x-x_0)/\hbar]$ determines the initial velocity v of the centre of the wavepacket.

There is an important difference between this collision problem and that of the α decay of the main text. The time derivative of the expectation value $\langle\psi_{\mathrm{B}}|x|\psi_{\mathrm{B}}\rangle$ remains approximately equal to v throughout the collision process that we consider. This is in contrast to $(\mathrm{d}/\mathrm{d}t)\langle\psi_\alpha|x_\alpha|\psi_\alpha\rangle$ of (2.23), which is much smaller than v in the early stage of the decay process.

In the numerical work of this appendix we use atomic units such that $\hbar = e^2 = a_0 = 1$ and $c = 137$ where a_0 is the Bohr radius. For the parameters of the model we choose $\epsilon_1 = 0$,

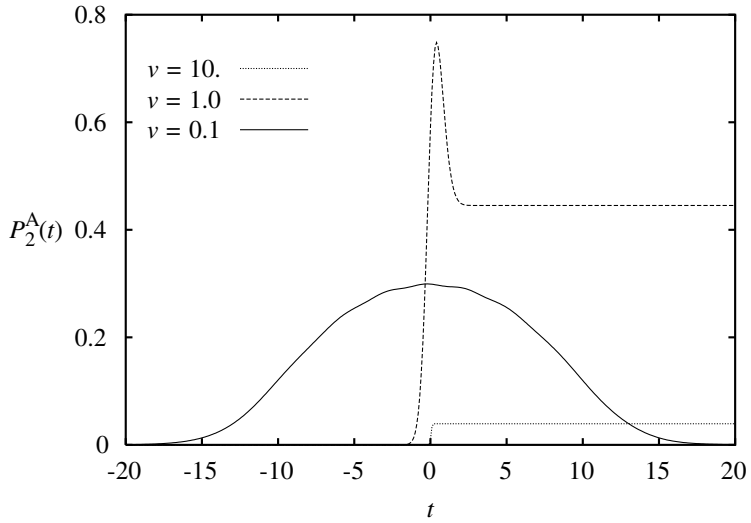

Figure B.1. Transition probabilities from state 1 to 2 as a function of time using model A for three different velocities of the projectile. The parameters are $\epsilon_1 = 0$, $\epsilon_2 = 1$, $\lambda = 1$, $g = 2$ and $m = 100$.

$\epsilon_2 = 1$, $\lambda = 1$, $g = 2$ and $m = 100$. The projectile is heavy in terms of the excitation energy: $mc^2 = 1.37^2 \times 10^6$. In fact, its mass is 100 times the mass of the electron. We did not make it as heavy as the α particle for computational convenience. For v we take three values, 0.1, 1 and 10. The kinetic energy of the incident particle $\frac{1}{2}mv^2$ is equal to the excitation energy 1 when $v = \sqrt{2} \times 0.1$. For the initial width of the wavepacket w_0 we take values between 1 and 10. We calculate the probability of finding the transition probability $P_2(t)$ for models A and B.

Figure B.1 shows the transition probability obtained in model A with various values of v. Note that $P_2^A(\infty)$ approaches zero as v becomes small. When $v = 0.1$ we find $P_2^A(\infty) \ll 1$, which means that the process becomes almost adiabatic.

We repeated the calculations for model B with the same values of v and a few different values of the width w_0 between 1 and 10. We found interesting similarities as well as differences between models A and B. The t dependence of $P_2^B(t)$ in the transient period varies depending on w_0. Its peak around $t = 0$ becomes broader as w_0 is increased. $P_2(\infty)$ is however remarkably insensitive to w_0. (This is interesting in the context of the wavepacket formalism of scattering theory, which we consider in more detail elsewhere.) As far as $P_2(\infty)$ is concerned the difference between models A and B is unimportant provided that the same value of v is used for the two models.

Returning to the discussion of the atomic ionization caused by the nuclear α decay, we recall that the effect on the atom is much smaller in models of type II as compared with those of type I. There are two conceivable reasons for the difference, which are respectively associated with the following two aspects. In models of type II the α wavefunction is such that (i) it is spread out over a very large space region of the order of $\hbar v/\Gamma$ and (ii) the average velocity $(\mathrm{d}/\mathrm{d}t)\langle x_\alpha \rangle$ of (2.23) is much smaller for most of the time than the classical velocity v_α of model I. Of course these two aspects are closely related to each other. Since we find in this appendix that the excitation due to a collision, namely, $P_2(\infty) \ll 1$, when v is very small, this suggests that aspect (ii) is much more important than aspect (i). Recall also the situation

pointed out below (2.24), namely, that, by the time when the average velocity increases toward the end of the decay process, the amplitude of the α-particle wavefunction in the atomic region has become very small.

References

[1] Migdal A 1941 *J. Phys. (USSR)* **4** 449
[2] Levinger J S 1953 *Phys. Rev.* **90** 11
[3] Fishbeck H J and Freedman M S 1975 *Phys. Rev. Lett.* **34** 173
Fishbeck H J and Freedman M S 1977 *Phys. Rev.* A **15** 162
[4] Gamow G 1928 *Z. Phys.* **51** 204
[5] Condon E U and Gurney R W 1928 *Nature* **112** 439
Condon E U and Gurney R W 1929 *Phys. Rev.* **33** 127
[6] Pöschl G and Teller F 1933 *Z. Phys.* **83** 143
[7] Flügge S 1974 *Practical Quantum Mechanics* (Berlin: Springer) p 94
[8] Lapidus L 1975 *Am. J. Phys.* **43** 790
[9] Nogami Y, Vallières M and van Dijk W 1976 *Am. J. Phys.* **44** 886
[10] Andrews 1976 *Am. J. Phys.* **44** 1064
[11] Goldberg A, Schey H M and Schwartz J L 1967 *Am. J. Phys.* **35** 177
[12] Bonche P, Koonin S and Negele J M 1976 *Phys. Rev.* C **13** 1226
[13] Galbraith I, Ching Y S and Abraham E 1984 *Am. J. Phys.* **52** 60
[14] Kataoka F 1998 *MSc Thesis* McMaster University, Hamilton (unpublished, available from the McMaster University library)
[15] van Dijk W, Kataoka F and Nogami Y 1999 *J. Phys. A: Math. Gen.* **32** 6347
[16] van Dijk W and Nogami Y 1999 *Phys. Rev. Lett.* **83** 2867
[17] French A P and Taylor E F 1979 *An Introduction to Quantum Mechanics* (New York: Norton) p 407
[18] Révai J and Nogami Y 1992 *Few-Body Systems* **13** 75
[19] Baur G, Rösel F and Trautmann D 1983 *J. Phys. B: At. Mol. Phys.* **16** L419
[20] D'Arrigo A, Eremin N V, Fazio G, Giardina G, Glotova M G, Klochko T V, Sacchi M and Taccone A 1994 *Phys. Lett.* B **332** 25
[21] Kasagi J, Yamazaki H, Kasajima N, Ohtsuki T and Yuki H 1997 *Phys. Rev. Lett.* **79** 371
Kasagi J, Yamazaki H, Kasajima N, Ohtsuki T and Yuki H 1997 *J. Phys. G: Nucl. Part. Phys.* **23** 1451
[22] Bertulani C A, de Paula D T and Zelevinsky V G 1999 *Phys. Rev.* C **60** 03162